

Self-trapping at the liquid-vapor critical point

Bruce N. Miller

*Department of Physics,
Texas Christian University,
Fort Worth, Texas 76129*

Terrence L. Reese

*Department of Physics,
Southern University and A&M College,
Baton Rouge, Louisiana 70813*

(Dated: November 14, 2018)

Abstract

Experiments suggest that localization via self-trapping plays a central role in the behavior of equilibrated low mass particles in both liquids and in supercritical fluids. In the latter case, the behavior is dominated by the liquid-vapor critical point which is difficult to probe, both experimentally and theoretically. Here, for the first time, we present the results of path-integral computations of the characteristics of a self-trapped particle at the critical point of a Lennard-Jones fluid for a positive particle-atom scattering length. We investigate the influence of the range of the particle-atom interaction on trapping properties, and the pick-off decay rate for the case where the particle is ortho-positronium.

PACS numbers: 02.70.Ss, 05.70.Jk, 14.60.cd

Keywords: Path Integral Monte Carlo, Critical Point Phenomena, Self-trapping, Electrons, Positrons, Positronium

The system consisting of a massive particle equilibrated in a host fluid, known to physicists and chemists as Brownian Motion, has played a seminal role in the development of Statistical Physics [1, 2]. However, the opposite regime of an equilibrated low mass particle is equally challenging and manifests a richer set of behaviors [3]. Except at very high temperatures, quantum mechanics is required to model the low mass particle. Possible quantum particle (qp) candidates are an electron, positron, or positronium atom, while the host can either be a dense gas or liquid below the critical temperature, or a supercritical fluid above it. Experimental measurements of the properties of a low mass particle equilibrated in a fluid strongly suggest that it can induce a local, mesoscopic, deformation in the fluid in which the qp becomes self-trapped, or localized. [3, 4] Since the qp has a long deBroglie wavelength, intuitively we anticipate that it simultaneously interacts with a large group of atoms or molecules in the host fluid forming a mesoscopic region of altered fluid density. Depending on whether the effective qp-atom interaction is attractive or repulsive, the local density of the host is either augmented or suppressed near the qp, resulting in the formation of either a "microdroplet" or "microbubble". The intuitive picture is completed by imagining that the qp occupies the ground state of the potential well induced by the formation of the density inhomogeneity, i.e. the droplet or bubble, thus stabilizing the deformation.

The positron-atom interaction is characterized by a negative scattering length so the experimental manifestation of self-trapping is a decrease in the positron lifetime due to the increase in the local electron density resulting from the formation of a droplet. The reverse is true for ortho-positronium. Angular momentum conservation eliminates the two photon decay process for the triplet state. As a result of the long natural lifetime of o-Ps in the vacuum, about 142 ns [4], its positron can annihilate more readily with an atomic electron of the host. A consequence of the fermionic repulsion between the electron in o-Ps and the electrons of the host fluid is that this "pick-off" annihilation rate is reduced when self-trapping occurs, demonstrating bubble formation [4]. Depending on the choice of the host, the electron-atom scattering length can have either sign, so each behavior is possible. While the most dramatic manifestation of self-trapping of the positron or positronium is a significant deviation from linearity in Arrhenius plots of the decay rate versus average density, the signature of electron self-trapping is a change in mobility [5].

In addition to the liquid state [6], self-trapping occurs in a broad, super-critical region of density, ρ , and temperature, T , surrounding the liquid-vapor critical point (ρ_c, T_c) [4, 7].

Since the isothermal compressibility diverges at the critical point, this is not surprising: The qp can more easily alter the local density in this region of temperature and density. However, as a result of the large density gradient induced by the earth's gravitational field, there are few reliable experimental studies of self-trapping close to the critical point [8]. Thus, although it dominates the self-trapping regime above T_c , the effect of close proximity to the critical point on self-trapping is not generally known [8].

The theory of self-trapping has evolved through different stages: In the earliest models, the qp occupies the ground state of a spherical step potential which is assumed to be proportional to the local fluid density [9]. In modelling the qp-host interaction the atomic nature of the host is ignored, and it is simply represented by a type of jellium. By minimizing the free energy of the qp-fluid system, it is possible to show that the deformation is stable in a bounded region of temperature and density near the critical point [9]. Later versions of mean field theory (MFT) permitted a continuous density profile [7, 10] and took into account the atomic nature of the host at an intermediate level [11]. An interesting improvement was obtained by employing the Percus-Yevick equation to include the effect of qp-atom and atom-atom correlations in the mean field formalism [12]. An advantage of MFT is that computations are reduced to numerically integrating a pair of coupled ordinary differential equations. However, in practice, they have only proved useful for fluids at low temperatures [7, 10, 12, 13]. This problem may arise because mean field theories only include a single bound state for the qp. More microscopically complete models have evolved during the last few decades based on the Feynman/Kac path integral [14] which overcome the major shortcomings of the earlier work. These account for the details of the qp-atom interaction and implicitly take into account local fluctuations in the disturbed fluid and the state of the qp. Two approaches have been employed, one based on an approximate analytic model requiring an educated choice of closure [15, 16], and the more direct alternative using Monte Carlo algorithms [13, 17]. While the latter avoids approximation, the computational cost is greater.

Here we employ path integral Monte Carlo (PIMC) to investigate self-trapping at the liquid-vapor critical point. We take advantage of recent improvements in fluid equilibrium theory which give accurate critical point parameters for the Lennard-Jones (6,12) potential.[18?] We model the qp-atom interaction with a hard-sphere potential and study the dependence of the physical and statistical properties of self-trapping on the hard sphere

diameter, R_{hs} . In particular, we investigate the dependence on R_{hs} of both the spreading of the qp wavefunction and its influence on the local deformation of the fluid. Since a repulsive qp-atom interaction is representative of positronium [4], we also estimate the pick-off annihilation rate for a simplified model of the atomic charge distribution.

Although no experimental measurements of the pick-off decay rate have been carried out precisely at the critical point, for the case of Xenon they exist for two supercritical temperatures, $300K$ and $340K$, over a large density range and strongly suggest the existence of the Ps self-trapped state [19]. In previous work [20] we have used PIMC to carry out simulations of Ps in Xenon at these temperatures, so it is natural to select the critical point of Xenon as a test case and a mass of $2m_e$ for the qp. The truncated version of the Lennard-Jones 6-12 potential was chosen to represent the inter-atomic potential. Wilding has established numerically accurate connections between the L-J distance and energy parameters (σ and ε) and the critical temperature and density (T_c and ρ_c), namely $\rho_c\sigma^3 = 0.3197$ and $kT_c/\varepsilon = 1.1876$ [18]. The experimental values of the critical density and temperature of Xenon are $T_c = 289K$ and $\rho_c = 5.299 \times 10^{-3}$ atoms/ \AA^3 yielding $\sigma = 3.92\text{\AA}$ and $\varepsilon/k = 243.5K$.

The computational simulation of the qp-fluid system using a complete quantum mechanical description would be intractable; thus approximate representations of the system are required. Except at very low temperatures, the translational degrees of freedom of an atomic fluid can be approximated with classical mechanics. Thus the qp-fluid system is well represented by a hybrid classical-quantum Hamiltonian:

$$H = \sum_1^N \mathbf{P}_j^2/2M + \sum_{N \geq j > k \geq 1} U(|\mathbf{R}_j - \mathbf{R}_k|) + H_{qp}, \quad H_{qp} = -\frac{\hbar^2}{2m} \Delta + \sum_1^N V(|\mathbf{r} - \mathbf{R}_j|). \quad (1)$$

Here \mathbf{P}_j and \mathbf{R}_j are the momenta and positions of the N host atoms, \mathbf{r} is the position of the qp, while U and V are the pairwise additive atom-atom and qp-atom interaction potentials. This is known as the adiabatic formulation and results in a hybrid partition function, [20]

$$Z = \int d\mathbf{R} e^{-\beta U(\mathbf{R})} \int d\mathbf{r} \langle \mathbf{r} | e^{-\beta H_{qp}} | \mathbf{r} \rangle / (N! \Lambda^{3N}), \quad (2)$$

where here \mathbf{R} represents $\{\mathbf{R}_j\}$, the complete $3N$ dimensional configuration space of the atoms with classical potential energy $U(\mathbf{R})$, and Λ is the atomic thermal wavelength. Thus, in principle, the quantum statistical average of the physical operator O can be computed from

$$\langle O \rangle = \int d\mathbf{R} e^{-\beta U(\mathbf{R})} \int d\mathbf{r} \langle \mathbf{r} | e^{-\beta H_{qp}} O | \mathbf{r} \rangle / (N! \Lambda^{3N} Z). \quad (3)$$

To obtain a formulation which is useful for computation, we follow the Feynman-Kac path integral construction [14]. First, by applying the Trotter formula to Z , we can express the trace over \mathbf{r} as a sum over discretized paths of P steps. For sufficiently large P the kinetic and potential energy operators approximately commute in each step, yielding the following expression for the partition function;

$$Z_P = \int d\mathbf{R} e^{-\beta U(\mathbf{R})} \left[\prod_0^{P-1} \int d\mathbf{r}_i e^{-P|\mathbf{r}_i - \mathbf{r}_{i+1}|^2/2\lambda^2} \rho(\mathbf{r}_i, \mathbf{r}_{i+1}, \mathbf{R}, \beta/P) \right], \quad (4)$$

where λ is the qp thermal wavelength. If we take ρ to be $\exp(-\beta V/P)$, equation (4) is known as the primitive approximation. Thus, in the discretized Feynman-Kac path integral [14], the qp is represented by a closed chain of P classical "pseudo-particles", or "slices" in imaginary time $t_i = (i/P)\beta\hbar$, with harmonically coupled nearest neighbors. Each pseudo-particle in the chain interacts with each atom through the potential V/P . The chain is equilibrated in a fluid at the augmented temperature PT [17, 21]. In the limit $P \rightarrow \infty$ the correspondence is exact. The spread of the chain corresponds to the uncertainty in position of the qp. The equivalence allows Monte Carlo methods developed for classical systems to be used to compute quantum mechanical equilibrium properties. Path integral Monte Carlo has been used successfully by many groups, including our own, to compute the equilibrium properties of quantum systems [22].

To insure convergence, while maintaining a constant temperature and average atomic density, the system size, the number of chain-particles P , and the number of statistical samples are increased until there are no significant changes in the calculated equilibrium properties. The algorithm we employed here depends on five parameters, the density, temperature, R_{hs} , the number of fluid atoms, N , and P . Convergence was improved by using an image potential to smooth out the singularity of the hard sphere, qp-atom interaction [20, 23]. A complete description of this method is given in our previous publications (see [20] and references cited within). For this initial study we selected three values of R_{hs} ; 0.5\AA , 5.0\AA and 9.5\AA while P was chosen to be 2000 as in our previous computations [20]. Since most of the cpu time was expended on repositioning the atoms, the large value of P did not pose a problem and insured convergence. To minimize edge effects, the length of the box in which the simulations were carried out was set to three times the qp thermal wavelength.

Important characteristics of the qp are the root mean square displacement ($D(t)$) between two particles along the chain separated by imaginary time t , and the density of chain particles

a distance r from its center of mass ($\rho_{cm}(r)$). D and ρ_{cm} are both direct measures of self-trapping. In an extended state the displacement between particles separated by t increases with t , reaching a maximum at $t = P/2$, according to a unimodal parabolic distribution. However, in a self-trapped state the chain is highly confined and thus, except for values of t near the end points at 0 and P , $D(t)$ is roughly constant. The function $\rho_{cm}(r)$ represents the mean probability density of the qp wavefunction, and becomes more peaked around the chain com as the chain becomes confined within its self-trapped bubble. A detailed discussion of these quantities and how they are computed can be found in our previous paper on self-trapping of Ps in Xenon [20].

Figure 1 is a plot of D versus t for the three R_{hs} values considered here. As R_{hs} increases, the figure shows that the shape of the plots changes from parabolic, corresponding to a nearly free particle, to one that is essentially constant in the central region, indicating that the chain becomes more confined [17, 21]. Increasing the value of R_{hs} expels fluid atoms from the vicinity of the chain particles into regions which don't overlap with them. At the same time the pressure applied by the fluid atoms compresses the chain. Since there are no repulsive forces between the pseudo-particles comprising the chain, their density near the chain com can become quite large. This can be seen in Figure 2, a plot of ρ_{cm} versus distance from the com, for the same R_{hs} values shown in Figure 1.

Information concerning the local deformation of the fluid induced by the qp is provided by the chain-fluid and com radial distribution functions, $g_{fp}(r)$, $g_{fcm}(r)$, yielding, respectively, the mean local density of fluid atoms a distance r from a chain pseudo-particle, and the chain center of mass. As usual, they are normalized to unity in the large r limit. In earlier work we showed that the former can be used to directly determine the o-Ps pick-off decay rate [20], while the latter provides direct evidence of self-trapping. In an extended state fluid atoms are able to penetrate into the vicinity of the chain com indicating that the qp is relatively spread out. On the other hand, in a completely self-trapped state, ground state dominance prevails, the chain is folded upon itself within the volume of the bubble, and fluid atoms are totally expelled from this region. $g_{fcm}(r)$ can be used to directly compute the average number of fluid atoms excluded from the vicinity of the chain. Figure 3, a plot of g_{fcm} versus position, indicates the strong exclusion of the fluid atoms from the vicinity of the chain at the largest value of R_{hs} . The significant value of ρ_{cm} at the origin for the smallest value of R_{hs} provides evidence that the atoms can penetrate the trapping region

and suggests that the qp is in an extended state. This is supported by the parabolic shape of $D(t)$. Hints of slow oscillation on large scales, which we are unable to resolve with the present system size, can be seen in Figure 3. An open question is whether these are simply finite size effects or represent a coupling between the correlation length of the fluid and the thermal wavelength of the qp. In our earlier work [20] short range oscillations occurred in ρ_{cm} over distances on the order of R_{hs} at $\rho = 2\rho_c$, indicating stacking of the fluid atoms in layers around the qp com. We see from the figure that at the critical point they are absent.

From g_{fcm} we found that the volume of the excluded fluid atoms from the trapping region is at least twice as great for $R_{hs} = 9.5\text{\AA}$ than for either 0.5\AA or 5.0\AA . Since increases in R_{hs} will lead to decreases in the number of fluid valence electrons near the qp available for annihilation, for the case where the qp is o-Ps the pick-off decay rate is expected to decrease with increasing R_{hs} . We computed the decay rate at the three values of R_{hs} considered above (see table I). Taking ratios, we found an approximately exponential decrease with R_{hs} with a characteristic length of 1.61\AA . In this model the Ps atom is treated as a composite particle in its *internal* hydrogenic ground state with an exponentially decreasing wavefunction representing the spread of the positron from the Ps center of mass. This is justified by the small ratio, $\approx 4 \times 10^{-3}$, of kT_c to the positronium excitation energy. For simplicity, the electron density around the host fluid atoms is modelled as a delta function. Thus the decay rate is dependent upon both the portion of the positron ground state wavefunction that manages to leak beyond R_{hs} and the number of fluid atoms centers it overlaps. The exponential decrease in the decay rate with increasing R_{hs} results from the decrease in both the density of fluid atoms and the amplitude of the positron wavefunction in the shell surrounding the hard sphere surface.

In contrast with mean field models, the power of PIMC is that it reveals the complete picture of both the distribution over qp quantum states and the response of the fluid to the qp "impurity". In general we have found that compared with a liquid [6] and our own PIMC computations at higher density [20], the mesoscopic region in which the qp is localized is much larger at the critical point. Moreover, the density profile of the fluid has a different shape - the "walls" are not nearly as steep and the structure is less sharply defined, i.e. it is *soft*. Our PIMC calculations for a supercritical fluid with $\rho = \rho_c$, but at higher temperature, show similarities with the critical point, but the behavior is less extreme [20].

In future work we plan to employ PIMC to directly evaluate the density of states. This

TABLE I: Natural log of the decay rate for three hard sphere diameters.

R_{hs} (Å)	Ln(Decay Rate)
0.5	-3.0
5.0	-20.0
9.5	-37.0

will enable us to determine the angular distribution of the annihilation photons from para-positronium, which can be directly compared with experiment. To date this has only been approached with a semi-empirical formulation of mean field theory [6]. It will be interesting to see what changes result from an ab initio computation which completely includes the effects of correlated fluctuations.

Acknowledgments

The authors benefitted from the support of the Research Foundation and the Division of Information Services of Texas Christian University. They are also grateful for the computer expertise provided by Peter Klinko and John Hopkins.

-
- [1] A. Einstein, *Theory of Brownian Motion* (Methuen, New York, 1926).
 - [2] E. W. Montroll and M. F. Schlesinger, in *Studies in Statistical Mechanics*, edited by J. Lebowitz and E. W. Montroll (North-Holland, Amsterdam, 1984).
 - [3] J. Hernandez, *Reviews of Modern Physics* **63**, 675 (1991).
 - [4] I. M. Charlton and J. W. Humbertson, *Positron Physics* (Cambridge, New York, 2001).
 - [5] A. F. Borghesani and M. Santini, *Phys. Rev. E* **65**, 056403 (2002).
 - [6] D. Dutta, B. N. Gunguly, D. Ganggopadhyay, T. Mukherjee, and B. Dutta-Roy, *Phys. Rev. B* **65**, 094114 (2002).
 - [7] I. T. Iakubov and A. G. Khrapak, *Rep. Prog. Phys.* **45**, 697 (1982).
 - [8] S. C. Sharma, S. R. Kafle, , and R. S. Surenda, *Phys. Rev. Lett.* **52**, 2233 (1984).
 - [9] R. A. Ferrell, *Phys. Rev.* **110**, 1355 (1958).

- [10] M. J. Stott and E. Zaremba, *Phys. Rev. Lett.* **38**, 1493 (1977).
- [11] R. M. Nieminen, M. Manninen, I. Vaimaa, and P. Hautojarvi, *Phys. Rev. A* **21**, 1677 (1980).
- [12] X. Yan and S. Tsai, *Phys. Rev. A* **46**, 4704 (1992).
- [13] T. Reese and B. N. Miller, *Phys. Rev. A* **39**, 4735 (1989).
- [14] R. P. Feynman, *Statistical Mechanics* (Addison-Wesley, Reading, MA, 1972).
- [15] D. Chandler, Y. Singh, and D. M. Richardson, *J. Chem. Phys.* **86**, 1075 (1984).
- [16] J. Chen and B. N. Miller, *Phys. Rev. B* **49**, 15615 (1994).
- [17] D. F. Coker, B. J. Berne, and D. Thirumalai, *J. Chem. Phys.* **86**, 5689 (1987).
- [18] N. B. Wilding, *J. Chem. Phys.* **52**, 602 (1995).
- [19] M. Tuomisaari, K. Rytola, and P. Hautojarvi, *J. Phys. B* **21**, 3917 (1988).
- [20] T. L. Reese and B. N. Miller, *Phys. Rev. E* **64**, 061201 (2001).
- [21] M. Sprik, M. L. Klein, and D. Chandler, *Phys. Rev. B* **31**, 4234 (1985).
- [22] V. A. Antonov, in *Quantum Monte Carlo Methods in Physics and Chemistry, NATO Science Series vol. 525*, edited by M. P. Nightingale and C. J. Umrigar (Kluwer, Boston, MA, 1999).
- [23] P. A. Whitlock and M. H. Kalos, *J. Chem. Phys.* **30**, 361 (1978).

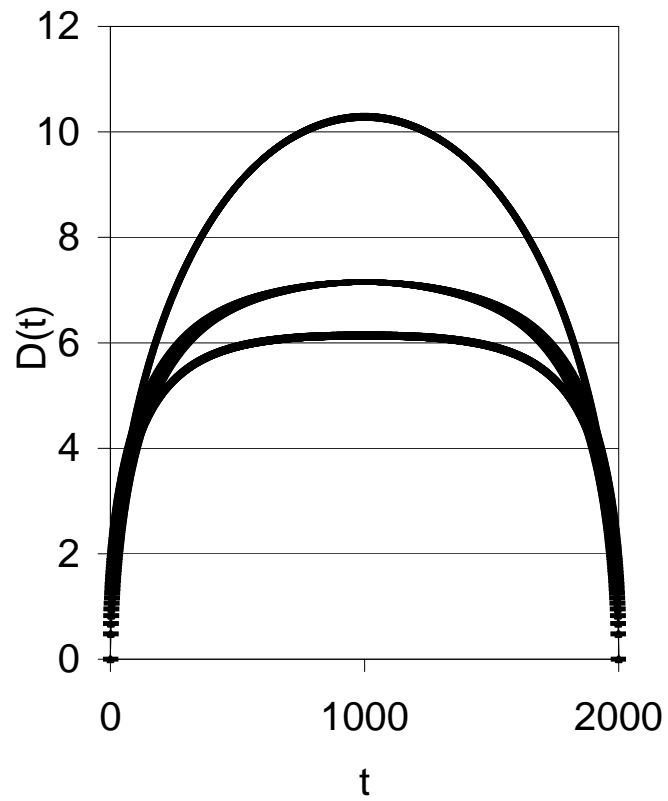


FIG. 1: Plot of $D(t)$ (Angstroms) versus t for the R_{hs} values 0.5\AA (upper curve), 5.0\AA (middle) and 9.5\AA (bottom).

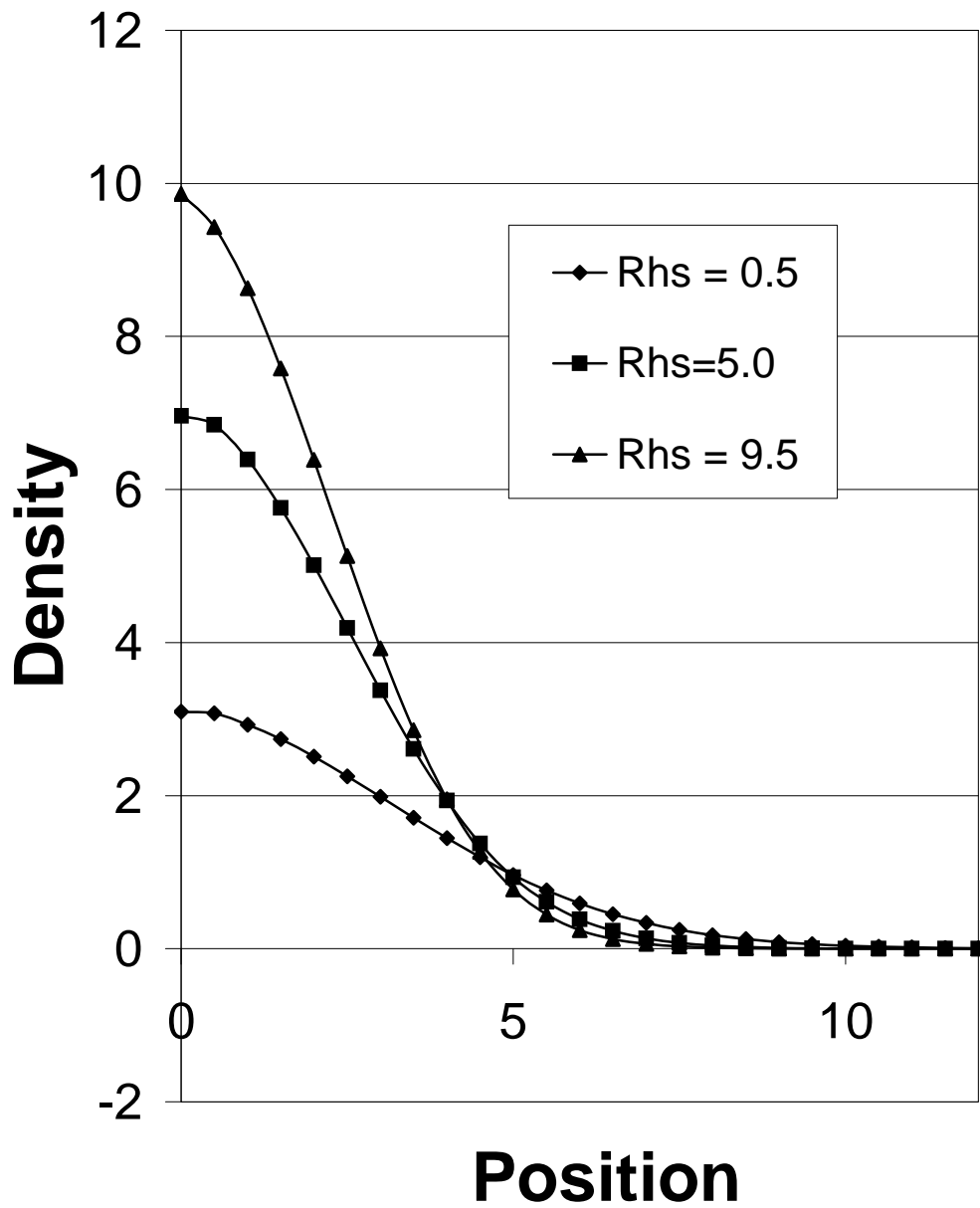


FIG. 2: Density of chain particles as a function of distance from the chain centroid, $\rho_{cm}(r)$, for the smallest (0.5\AA), average (5.0\AA), and largest (9.5\AA) values of R_{hs} .

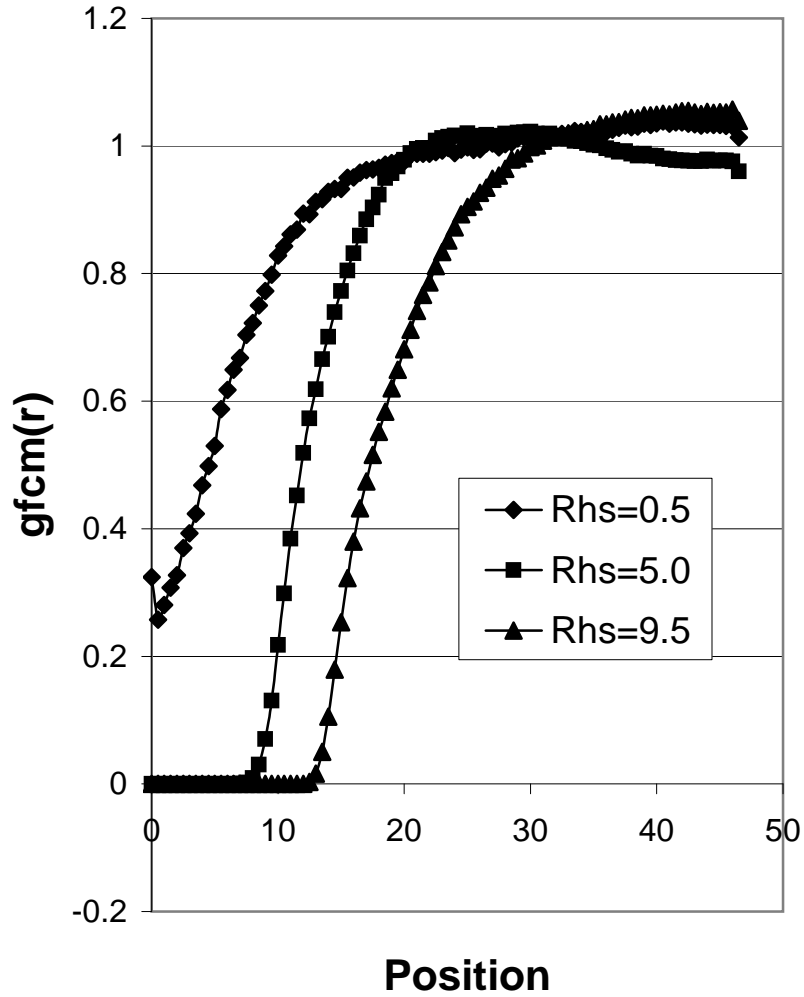


FIG. 3: Density of fluid atoms from the chain center of mass, $g_{fcm}(r)$, versus position for the smallest (0.5 Å), average (5.0 Å), and largest (9.5 Å) values of R_{hs} .